Composites Communications 1 (2016) 15–19

Contents lists available at ScienceDirect

Composites Communications

journal homepage: www.elsevier.com/locate/coco

Nanocubic-Co_3O_4 coupled with nitrogen-doped carbon nanofiber network: A synergistic binder-free catalyst toward oxygen reduction reactions

Yue-E Miao [a], Fei Li [a], Hengyi Lu [b], Jiajie Yan [b], Yunpeng Huang [b], Tianxi Liu [a,b,*]

[a] State Key Laboratory for Modification of Chemical Fibers and Polymer Materials, College of Materials Science and Engineering, Donghua University, Shanghai 201620, China

[b] State Key Laboratory of Molecular Engineering of Polymers, Department of Macromolecular Science, Fudan University, Shanghai 200433, China

ARTICLE INFO

Article history:
Received 27 January 2016
Received in revised form
13 June 2016
Accepted 7 July 2016
Available online 20 August 2016

Keywords:
Nanocubic-Co_3O_4
Nitrogen-doped carbon nanofiber
Binder-free
Oxygen reduction reactions

ABSTRACT

High-performance electrocatalysts with excellent catalytic activity and long durability competitive to Pt are urgently necessary for fuel cell development. Here, a novel self-standing membrane of nitrogen-doped carbon nanofibers (NCNF) has been developed, acting as a three-dimensionally networked and conductive template for immobilization of electrochemically active Co_3O_4 particles. Thus, nanocubic-Co_3O_4 coated NCNF (NCNF@Co_3O_4) composite fiber membrane with hierarchical structures is obtained, which subtly combines the synergistic effects between the electroactive nanocubic-Co_3O_4, efficient surface nitrogen doping and highly conductive NCNF network. Therefore, the NCNF@Co_3O_4 composite exhibits excellent catalytic activity toward oxygen reduction reactions with positive E_{peak} potential, high current density and superior durability over the commercial Pt/C catalyst, being a promising noble metal-free catalyst for practical fuel cell applications.

1. Introduction

The increasing demand for clean and sustainable energy has inspired extensive exploration of advanced energy conversion and storage systems with high efficiency, low cost and environmental benignity, such as supercapacitors, lithium-ion batteries, fuel cells, and metal–air batteries [1,2]. Nevertheless, the sluggish kinetics of oxygen reduction reaction (ORR) on the cathode side definitely limits the successful commercialization of high efficiency fuel cells and metal–air batteries. Pt-based materials have been considered as the most active noble metal ORR electrocatalysts, but largely constrained in practical applications due to their scarcity, poor durability and severe crossover effects [3,4]. Therefore, non-precious metal-based and even metal-free electrocatalysts, such as transition metal oxides (TMOs), metal chalcogenides and carbon-based materials are newly emerging as promising candidates for high-performance fuel cell and metal–air battery applications [5–7].

Co_3O_4, as a typical kind of TMOs, has attracted increasing attention as a relatively active ORR catalyst with natural abundance, low cost, and environmental compatibility [8–10]. Nevertheless, poorly conductive Co_3O_4 nanoparticles always suffer from inevitable dissolution and agglomeration during the reaction processes, thus leading to compromised kinetics and reduced ORR activity. Directly growing or immobilizing Co_3O_4 nanocrystals on various carbon-based supporting materials, like graphene, carbon nanotubes (CNTs) or porous carbon, is proved to be an effective strategy to construct hybrid materials with largely increased surface active sites, optimized electrical and chemical coupling between Co_3O_4 and the supporting substrates [11–13]. For example, N-doped graphene/Co_3O_4 composites [11], N-doped graphene/carbon nanotube/Co_3O_4 composites [14], and Co_3O_4 nanocrystals/O-/N-doped carbon nanowebs [15] have been demonstrated to show high activity and long-term stability as ORR catalysts. However, carbon-based nanoparticles like CNTs and graphene easily tend to restack or aggregate due to the strong van der Waals interactions between individual particles, which ultimately results in decreased surface area and electrochemical active sites to take part in efficient catalytic processes. For this reason, it is urgently needed to explore novel conductive carbon-based frameworks with synergistically enhanced mechanical stability and electrochemical performance.

Electrospinning is considered as a simple and versatile technique to produce self-standing carbon nanofiber membranes with unique three-dimensional (3D) fiber network, good structural stability and high flexibility [16–18]. The interconnected 3D macroporous architecture can act as a highly conductive core for fast

* Corresponding author.
E-mail addresses: txliu@dhu.edu.cn, txliu@fudan.edu.cn (T. Liu).

http://dx.doi.org/10.1016/j.coco.2016.07.003
2452-2139/

electron transport, as well as provide sufficient surface active sites for further immobilization of electrochemically active nanoparticles [19,20]. Herein, nitrogen-doped carbon nanofibers (NCNFs) have been facilely obtained through the combination of electrospinning, in-situ polymerization and high-temperature carbonization. Subsequently, the free-standing membrane of nanocubic-Co_3O_4 coated NCNF (NCNF@Co_3O_4) composite is fabricated via a simple hydrothermal reaction (Fig. S1), which combines the superior electroactivity of nanocubic-Co_3O_4, the efficient doping effect of nitrogen, and the good conductivity of NCNF network. Hence, the NCNF@Co_3O_4 composite membrane exhibits excellent catalytic performance toward oxygen reduction reactions, being a promising noble metal-free ORR catalyst in fuel cell applications.

2. Results and discussion

As shown in Fig. 1a, electrospun poly(amide acid)-derived carbon nanofibers (CNFs) show uniform diameter with an average size of about 140 nm. In order to introduce nitrogen into CNFs, in-situ polymerization of aniline was carried out in the presence of poly(amide acid) fiber template, followed by a high-temperature carbonization treatment. Under an initial aniline concentration of 0.02 M, nitrogen-doped CNFs (denoted as NCNF-0.02) are obtained, which exhibit an increased fiber diameter of about 215 nm with uniformly distributed needle-like nanoparticles on the fiber surface (Fig. 1b). Satisfyingly, the homogeneous bump structure of NCNF-0.02 can provide more catalytic active sites and be beneficial to faster ion diffusion compared with the smooth surface of CNFs. Subsequent deposition of Co_3O_4 nanoparticles was achieved by the hydrothermal reaction of cobalt acetate ($Co(OAc)_2 \cdot 4H_2O$) in the presence of NCNF-0.02 template. As expected, nanocubic-Co_3O_4 particles with a mean size of 20–30 nm are uniformly distributed on the surface of NCNF-0.02 at a proper concentration of $Co(OAc)_2 \cdot 4H_2O$, forming NCNF-0.02@Co_3O_4-0.2 composite fibers with an obvious coaxial structure (Fig. 1c), which can effectively prevent the severe agglomeration of Co_3O_4 powder as obtained in the absence of NCNF-0.02 template (Fig. 1d). Furthermore, the NCNF-0.02@Co_3O_4-0.2 composite fiber membrane exhibits distinct free-standing feature (as shown in the inset of Fig. 1c), coincidentally omitting the usage of insulating binders required for powdery materials and thus effectively avoiding unwanted inner resistance for oxygen reduction reactions.

The structure of CNF, NCNF-0.02, NCNF-0.02@Co_3O_4-0.2 fiber membranes, and Co_3O_4 powder was further investigated by X-ray diffraction (XRD) patterns. As shown in Fig. 2a, both of pure CNF and NCNF-0.02 fiber membranes exhibit amorphous structure while sharp peaks at $2\theta = 19.5°$, 31.6° and 37.2° are observed for NCNF-0.02@Co_3O_4-0.2 fiber membrane and Co_3O_4 powder, which correspond to the (111), (220) and (311) crystal facets of cubic Co_3O_4 with good crystalline structure.

X-ray photoelectron spectroscopy (XPS) characterization was carried out to further analyze the elemental composition of NCNF-0.02 and NCNF-0.02@Co_3O_4-0.2 fiber membranes. As shown in Fig. 2b, the survey spectrum of NCNF-0.02 indicates the existence of C, O and N elements, confirming the successful incorporation of nitrogen into the carbon nanofibers through the in-situ polymerization of aniline and carbonization process. The high-resolution XPS spectrum of N 1 s (Fig. 2c) reveals that nitrogen atoms exist in three

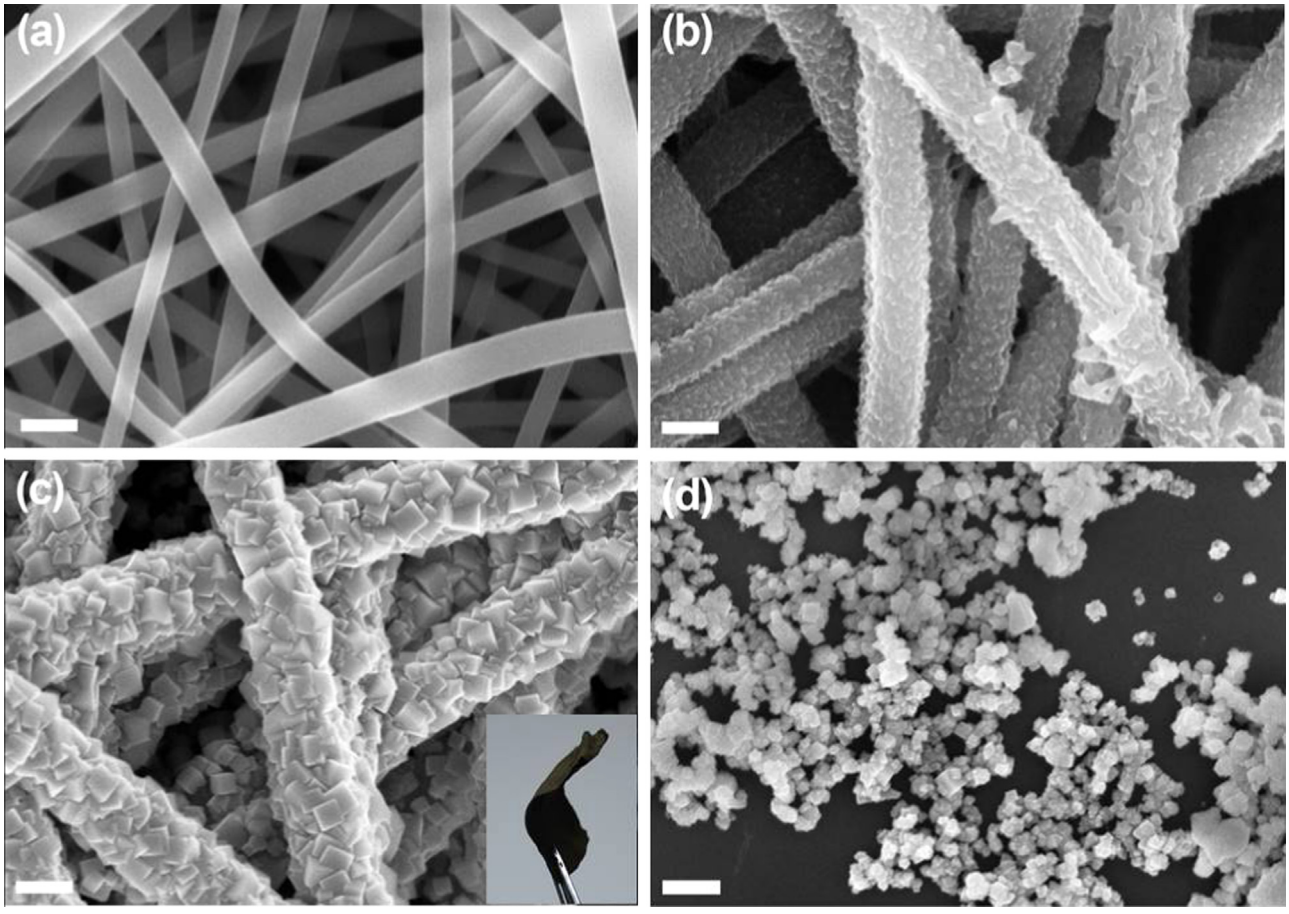

Fig. 1. FESEM images of electrospun CNF (a), NCNF-0.02 (b), NCNF-0.02@Co_3O_4-0.2 (c) fiber membranes, and Co_3O_4 powder (d). Scale bar: 100 nm. The inset of (c) shows the distinct free-standing feature of NCNF-0.02@Co_3O_4-0.2 fiber membrane.

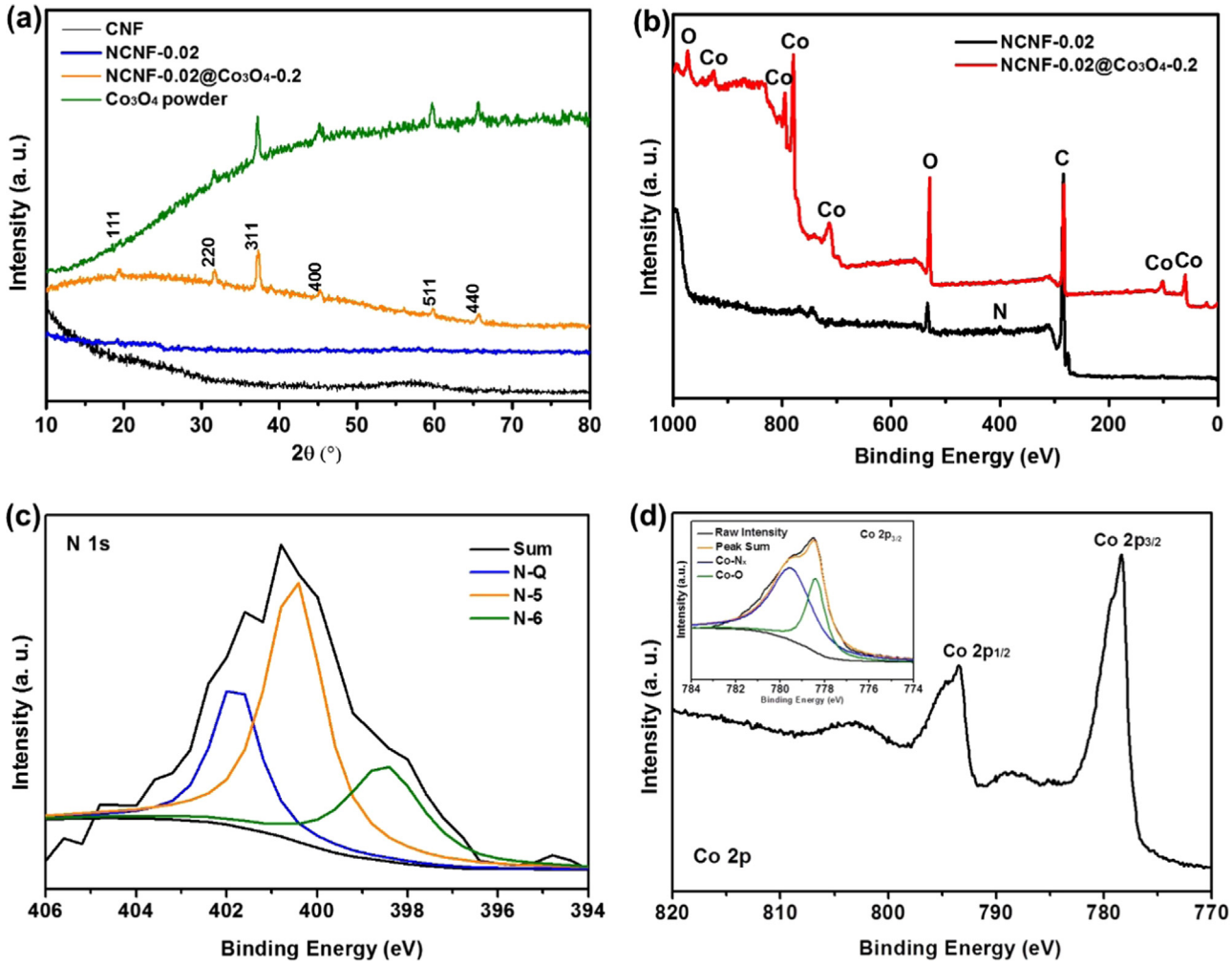

Fig. 2. (a) XRD patterns of electrospun CNF, NCNF-0.02, NCNF-0.02@Co_3O_4-0.2 fiber membranes, and Co_3O_4 powder; XPS spectra of NCNF-0.02 and NCNF-0.02@Co_3O_4-0.2 fiber membranes: (b) the survey scan, (c) N 1 s, and (d) Co 2p.

states, including pyridinic-N (N-6, 398.5 eV), pyrrolic-N (N-5, 400.5 eV) and graphitic-N (N-Q, 401.7 eV). Interestingly, pyridinic-N and graphitic-N are dominated in the XPS spectrum of N 1 s, which are reported to be beneficial to decreasing the onset potentials and improving the limited current density respectively [21,22]. Therefore, the NCNF-0.02 fiber membrane is proved to be a promising catalytic supporting material for oxygen reduction reactions. In addition, the survey spectrum of NCNF-0.02@Co_3O_4-0.2 fiber membrane indicates the existence of Co elements. As shown in the high-resolution Co 2p spectrum of Fig. 2d, two main peaks are observed at binding energies of 793.5 eV and 778.5 eV, which are assigned to Co $2p_{1/2}$ and Co $2p_{3/2}$, respectively, further demonstrating the successful acquisition of Co_3O_4 nanostructures on NCNF-0.02 fiber surface via the facile hydrothermal reaction. Moreover, Co $2p_{3/2}$ can be deconvoluted into two peaks at binding energies of 779.6 eV and 778.4 eV as shown in the inset of Fig. 2d, corresponding to the Co–N_x and Co–O bonds, respectively [23]. Especially, the coordination between Co and N indicated by the dominated Co–N_x bond is reported to be favorable for the improvement in electrocatalytic activity of NCNF-0.02@Co_3O_4-0.2 composite membrane [10].

The electrocatalytic ORR activity was first evaluated by cyclic voltammetry (CV) in O_2-saturated (solid line) and N_2-saturated (dash line) 0.1 M KOH aqueous solution at a scan rate of 5 mV s^{-1} (Fig. 3a). Well-defined cathodic reduction peaks can only be observed in the presence of O_2 for all samples. Unexpectedly, pure Co_3O_4 powder exhibits rather poor current response toward ORR with the E_{peak} potential at −0.37 V, which may be affected by the severe aggregation and poor conductivity of Co_3O_4 particles. In contrast, CNF fiber membrane with intertwined conductive network structure exhibits higher current response with an obvious E_{peak} potential at −0.35 V. Moreover, introducing nitrogen doping in NCNF-0.02 fiber membrane results in more positive E_{peak} potential (−0.24 V) with largely increased current density, further indicating that nitrogen doping can greatly enhance the catalytic activity of CNF. When Co_3O_4 is incorporated under a low initial molar weight (0.05 mmol) of $Co(OAc)_2$, nanocubic-Co_3O_4 particles with a mean size of 100 nm are sparsely scattered on NCNF-0.02 fiber membrane (Fig. S2a), resulting in slight positive shift of the E_{peak} potential (−0.21 V). With the molar weight further increased to 0.2 mmol, Co_3O_4 nanoparticles with smaller size of about 20-30 nm are uniformly distributed on NCNF-0.02 fiber surface (Fig. S2b), thus leading to more positive E_{peak} potential (−0.18 V) with higher current density, which outperforms most of the previously reported Co/carbon based catalysts as shown in Table S1. The outstanding catalytic performance can be attributed to the largely increased surface active sites of Co_3O_4 to take part in catalytic reactions, as well as the highly catalytic active environment constructed by the efficient chemical bonding (i.e., Co–O–C and Co–N–C) between C, O, N and Co atoms [11,24]. More interestingly, further increasing the molar weight of $Co(OAc)_2$ precursor leads to the formation of Co_3O_4 nanodisks accumulated by nanocubic particles of about 20-30 nm, which are all perpendicularly grown

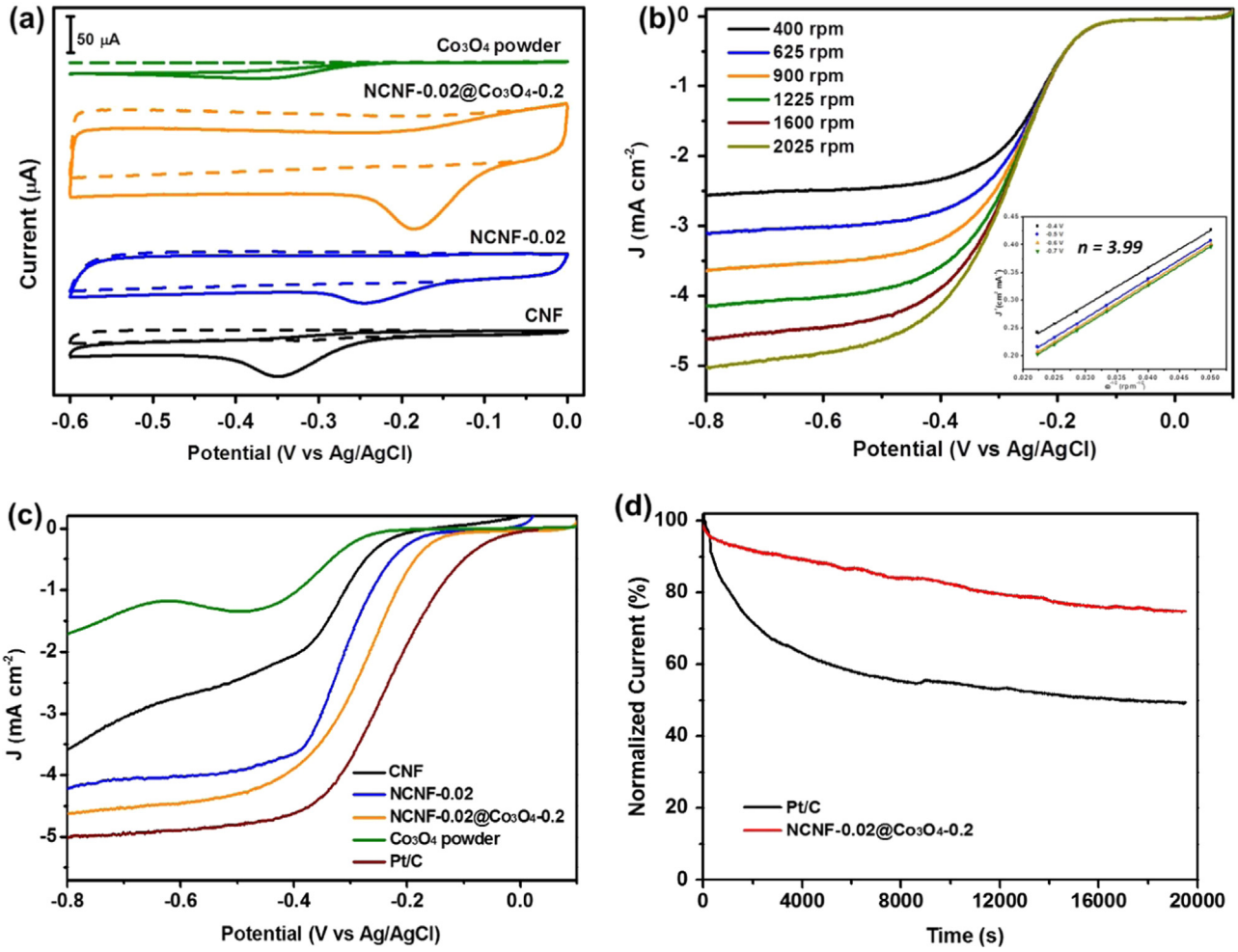

Fig. 3. (a) CV curves of electrospun CNF, NCNF-0.02, NCNF-0.02@Co_3O_4-0.2 fiber membranes, and Co_3O_4 powder electrodes in O_2-saturated (solid line) and N_2-saturated (dash line) 0.1 M KOH solution with a sweep rate of 5 mV s^{-1}; (b) Rotating-disk voltammograms, and the corresponding Koutecky-Levich (K–L) plots (J^{-1} *vs.* $\omega^{-1/2}$) of NCNF-0.02@Co_3O_4-0.2 composite fiber membrane electrode at different rotation rates in O_2-saturated 0.1 M KOH solution; (c) LSV curves of CNF, NCNF-0.02, NCNF-0.02@Co_3O_4-0.2 fiber membranes, Co_3O_4 powder and the commercial Pt/C electrode at the rotation rate of 1600 rpm in O_2-saturated 0.1 M KOH solution; (d) Chronoamperometric response of NCNF-0.02@Co_3O_4-0.2 composite fiber membrane and Pt/C electrode in O_2-saturated 0.1 M KOH solution.

on the surface of NCNF-0.02 fibers (Fig. S2c). Therefore, the NCNF-0.02@Co_3O_4-0.2 fiber membrane still keeps a positive E_{peak} potential (-0.19 V) with high current density.

To further investigate the electrocatalytic activity and reveal the kinetics of the NCNF-0.02@Co_3O_4-0.2 fiber membrane, linear sweep voltammetry (LSV) measurements were performed at various rotation speeds in O_2-saturated 0.1 M KOH solution. As shown in Fig. 3b, the current density of NCNF-0.02@Co_3O_4-0.2 fiber membrane modified rotating disk electrode (RDE) increases with increasing rotation rate from 400 to 2025 rpm, suggesting the shortened diffusion distance at high rotation speeds. According to previous reports [25], the electrochemical reduction of oxygen in basic solution mainly happens through two possible pathways, including the two-electron reduction pathway with OOH^- as an intermediate product and the four-electron pathway to produce OH^- which is considered as a more efficient approach to achieve maximum energy capacity. To better investigate the kinetic electron reaction mechanism, Koutecky–Levich (K–L) plots (J^{-1} *vs.* $\omega^{-1/2}$) of NCNF-0.02@Co_3O_4-0.2 composite electrode are obtained at various potentials (see SI for detailed calculation process), all of which exhibit good linearity and almost parallel with each other (the inset of Fig. 3b), suggesting that the ORR process follows the first-order reaction kinetics with respect to the concentration of dissolved oxygen. Correspondingly, the electron transfer number (n) is calculated to be 3.99 for NCNF-0.02@Co_3O_4-0.2 composite catalyst, indicating a preferred $4e^-$ oxygen reduction process. LSV curves for different catalysts including CNF, NCNF-0.02, NCNF-0.02@Co_3O_4-0.2 fiber membranes, Co_3O_4 powder and Pt/C were also obtained as shown in Fig. 3c. Compared with Co_3O_4 powder, CNF and NCNF-0.02 membranes exhibit lower onset potential and larger current density, which can be attributed to the good conductivity of the carbon nanofiber backbone, as well as the nitrogen-induced charge delocalization and high hydrophilicity for efficient oxygen absorption. Moreover, the novel construction of NCNF-0.02@Co_3O_4-0.2 composite with coaxial structures ultimately leads to the efficient coupling between nanocubic-Co_3O_4 and the NCNF-0.02 template, thus resulting in a more desirable four-electron pathway and largely improved electrocatalytic activity whose onset potential is much closer to that of the commercial Pt/C.

Long-term stability of the ORR catalyst is another important criterion for practical fuel cell applications. Hence, chronoamperometric measurement of NCNF-0.02@Co_3O_4-0.2 composite electrode was conducted at -0.4 V (vs Ag/AgCl) in O_2 saturated 0.1 M KOH at the rotation speed of 1600 rpm. As shown in Fig. 3d, the relative current of commercial Pt/C has a sharp drop of about 45% after 20,000 s, while the NCNF-0.02@Co_3O_4-0.2 composite still keeps a high retention of over 75%. The good long-term stability of NCNF-0.02@Co_3O_4-0.2 composite is attributed to the highly conductive NCNF nanofiber network, which can effectively suppress the structural collapse and active site dissolution of Co_3O_4.

3. Conclusions

In summary, a novel free-standing membrane consisting of nanocubic-Co_3O_4 coated NCNF composite fibers has been developed through the facile combination of electrospinning, in-situ polymerization and hydrothermal reaction. Notably, the NCNF template effectively provides a three-dimensional macroporous architecture, which not only acts as a highly conductive core for fast electron transfer, but also affords large surface area for further immobilization of electrochemically active nanocubic-Co_3O_4 particles. The obtained NCNF@Co_3O_4 composite exhibits excellent ORR catalytic activity with positive E_{peak} potential, high current density and superior durability over the commercial Pt/C catalyst. Therefore, this work presents a promising protocol for the large-scale production of noble metal-free ORR catalyst in practical fuel cell applications.

Acknowledgments

The authors are grateful for the financial support from the National Natural Science Foundation of China (51373037 and 51433001).

Appendix A. Supplementary material

Supplementary data associated with this article can be found in the online version at http://dx.doi.org/10.1016/j.coco.2016.07.003.

References

[1] A.L.M. Reddy, S.R. Gowda, M.M. Shaijumon, P.M. Ajayan, Hybrid nanostructures for energy storage applications, Adv. Mater. 24 (2012) 5045–5064.
[2] X. Chen, C. Li, M. Gratzel, R. Kostecki, S.S. Mao, Nanomaterials for renewable energy production and storage, Chem. Soc. Rev. 41 (2012) 7909–7937.
[3] GreeleyJ, I.E.L. Stephens, A.S. Bondarenko, T.P. Johansson, H.A. Hansen, T. F. Jaramillo, RossmeislJ, Chorkendorffl, J.K. Nørskov, Alloys of platinum and early transition metals as oxygen reduction electrocatalysts, Nat. Chem. 1 (2009) 552–556.
[4] B. Lim, M. Jiang, P.H.C. Camargo, E.C. Cho, J. Tao, X. Lu, Y. Zhu, Y. Xia, Pd-pt bimetallic nanodendrites with high activity for oxygen reduction, Science 324 (2009) 1302–1305.
[5] J. Masa, W. Xia, M. Muhler, W. Schuhmann, On the role of metals in nitrogen-doped carbon electrocatalysts for oxygen reduction, Angew. Chem. Int. Ed. 54 (2015) 10102–10120.
[6] L. Dai, Y. Xue, L. Qu, H.J. Choi, J.B. Baek, Metal-free catalysts for oxygen reduction reaction, Chem. Rev. 115 (2015) 4823–4892.
[7] G. Zhang, C. Li, J. Liu, L. Zhou, R. Liu, X. Han, H. Huang, H. Hu, Y. Liu, Z. Kang, One-step conversion from metal-organic frameworks to Co_3O_4@N-doped carbon nanocomposites towards highly efficient oxygen reduction catalysts, J. Mater. Chem. A 2 (2014) 8184–8189.
[8] J. Xu, P. Gao, T.S. Zhao, Non-precious Co_3O_4 nano-rod electrocatalyst for oxygen reduction reaction in anion-exchange membrane fuel cells, Energy Environ. Sci. 5 (2012) 5333–5339.
[9] Y.J. Sa, K. Kwon, J.Y. Cheon, F. Kleitz, S.H. Joo, Ordered mesoporous Co_3O_4 spinels as stable, bifunctional, noble metal-free oxygen electrocatalysts, J. Mater. Chem. A 1 (2013) 9992–10001.
[10] Y. Wang, Y. Nie, W. Ding, S.G. Chen, K. Xiong, X.Q. Qi, Y. Zhang, J. Wang, Z. D. Wei, Unification of catalytic oxygen reduction and hydrogen evolution reactions: Highly dispersive Co nanoparticles encapsulated inside co and nitrogen co-doped carbon, Chem. Commun. 51 (2015) 8942–8945.
[11] Y. Liang, Y. Li, H. Wang, J. Zhou, J. Wang, T. Regier, H. Dai, Co_3O_4 nanocrystals on graphene as a synergistic catalyst for oxygen reduction reaction, Nat. Mater. 10 (2011) 780–786.
[12] Y.Y. Liang, H.L. Wang, P. Diao, W. Chang, G.S. Hong, Y.G. Li, M. Gong, L.M. Xie, J. G. Zhou, J. Wang, T.Z. Regier, F. Wei, H.J. Dai, Oxygen reduction electrocatalyst based on strongly coupled cobalt oxide nanocrystals and carbon nanotubes, J. Am. Chem. Soc. 134 (2012) 15849–15857.
[13] C. Zhang, M. Antonietti, T.P. Fellinger, Blood ties: Co_3O_4 decorated blood derived carbon as a superior bifunctional electrocatalyst, Adv. Funct. Mater. 24 (2014) 7655–7665.
[14] S.S. Li, H.P. Cong, P. Wang, S.H. Yu, Flexible nitrogen-doped graphene/carbon nanotube/Co_3O_4 paper and its oxygen reduction activity, Nanoscale 6 (2014) 7534–7541.
[15] L. Li, S. Liu, A. Manthiram, Co_3O_4 nanocrystals coupled with O- and N-doped carbon nanoweb as a synergistic catalyst for hybrid li-air batteries, Nano Energy 12 (2015) 852–860.
[16] Q.Y. Wu, H.Q. Liang, M. Li, B.T. Liu, Z.K. Xu, Hierarchically porous carbon membranes derived from PAN and their selective adsorption of organic dyes, Chin. J. Polym. Sci. 34 (2016) 23–33.
[17] Y.E. Miao, T.X. Liu, Recent progress in hierarchically organized polymer nanocomposites based on electrospun nanofibers, Acta Polym. Sinica 8 (2012) 801–811.
[18] J.J. Yan, H.Y. Lu, Y.P. Huang, J. Fu, S.Y. Mo, C. Wei, Y.E. Miao, T.X. Liu, Polydopamine-derived porous carbon fiber/cobalt composites for efficient oxygen reduction reactions, J. Mater. Chem. A 3 (2015) 23299–23306.
[19] D. Liu, X. Zhang, Z. Sun, T.Y. You, Free-standing nitrogen-doped carbon nanofiber films as highly efficient electrocatalysts for oxygen reduction, Nanoscale 5 (2013) 9528–9531.
[20] Y. Qiu, J. Yu, T. Shi, X. Zhou, X. Bai, J.Y. Huang, Nitrogen-doped ultrathin carbon nanofibers derived from electrospinning: Large-scale production, unique structure, and application as electrocatalysts for oxygen reduction, J. Power Sources 196 (2011) 9862–9867.
[21] S. Jiang, C. Zhu, S. Dong, Cobalt and nitrogen-cofunctionalized graphene as a durable non-precious metal catalyst with enhanced orr activity, J. Mater. Chem. A 1 (2013) 3593–3599.
[22] Y. Su, Y. Zhu, H. Jiang, J. Shen, X. Yang, W. Zou, J. Chen, C. Li, Cobalt nanoparticles embedded in N-doped carbon as an efficient bifunctional electrocatalyst for oxygen reduction and evolution reactions, Nanoscale 6 (2014) 15080–15089.
[23] Y. Jiang, Y. Lu, X. Wang, Y. Bao, W. Chen, L. Niu, A cobalt-nitrogen complex on N-doped three-dimensional graphene framework as a highly efficient electrocatalyst for oxygen reduction reaction, Nanoscale 6 (2014) 15066–15072.
[24] C. Sun, F. Li, C. Ma, Y. Wang, Y. Ren, W. Yang, Z. Ma, J. Li, Y. Chen, Y. Kim, L. Chen, Graphene-Co_3O_4 nanocomposite as an efficient bifunctional catalyst for lithium-air batteries, J. Mater. Chem. A 2 (2014) 7188–7196.
[25] D. Yu, Q. Zhang, L. Dai, Highly efficient metal-free growth of nitrogen-doped single-walled carbon nanotubes on plasma-etched substrates for oxygen reduction, J. Am. Chem. Soc. 132 (2010) 15127–15129.